A simplified optical millimeter-wave generation scheme based on frequency-quadrupling*

TAO Long-biao (陶隆彪), **GAO Hong-yun** (郜洪云)**, **DENG Shuo** (邓硕), **LÜ Hai-fei** (吕海飞), **WEN Xiao-yan** (文晓艳), **and LI Min** (黎敏)

Physical Department, College of Science and Technology, Wuhan University of Technology, Wuhan 430070, China

(Received 8 March 2019; Revised 17 April 2019)

This paper analyzes and demonstrates a simplified frequency quadrupling configuration for optical millimeter-wave (mm-wave) generation, in which the electrical phase shifter and optical filter are omitted. Theoretical analysis is given to reach the optimum operating conditions including direct current (DC) bias voltage, optical transmission point of the dual-parallel Mach-Zehnder modulator (MZM) bias voltage, optical transmission point of the dual-parallel Mach-Zehnder modulator (DP-MZM), amplitude of the radio frequency (RF) driving signal and the impact of the extinction ratio (*EF*) on the optical sideband suppression ratio (*OSSR*) and radio frequency spurious suppression ratio (*RFSSR*). Experiments prove an *OSSR* of 15 dB and an *RFSSR* of 26 dB for the new frequency quadrupling scheme at 6 GHz, 8GHz and 10 GHz of RF driving signal without any electrical phase shifter or optical filter. This system exhibits the advantage of low wavelength dependence and large frequency tunable range.

Document code: A **Article ID:** 1673-1905(2020)01-0007-5

DOI https://doi.org/10.1007/s11801-020-9036-y

Photonic generation of high frequency millimeter-wave (mm-wave) signal has attracted great interests for radio-over-fiber (ROF) link, broadband wireless communication systems, optical measurement, radars and terahertz applications[1-5]. Photonic generation of mm-wave takes the heterodyne scheme of two phase correlated optical signals and comes up with the beat wavelength at photodiode (PD). External modulation technique based on Mach-Zehnder modulators (MZMs) shows an outstanding potential to generate mm-wave signal among various approaches because of the wide frequency tunable range, high nonlinear efficiency, low phase noise and excellent system stability.

Various approaches based on MZMs have been reported in mm-wave signal generation. A single MZM biased at the carrier suppressed double sideband (CS-DSB) transmission point generates only frequency doubling signal[6]. Frequency quadrupling commonly requires two cascaded MZMs as well as an electrical phase shifter[7], or an integrated dual-parallel Mach-Zehnder modulator (DP-MZM) with an electrical phase shifter[8] only. Despite a few groups reported a frequency quadrupling configuration which the electrical phase and optical filter are omitted, there is a lack of a clear theoretical analysis and experimental results discussion[9]. All of the approaches are based on the inherent nonlinear response of MZM to generate high-order optical sidebands[10-12]. Several frequency 10 to 16-tupling optical millimeter-wave signal generation schemes are reported aiming at mm-wave signal generation, in which frequency multiplication is realized by involving nonlinear devices, such as semiconductor optical amplifier (SOA) or nonlinear optical fibers[13-15]. But electrical phase shifter and optical filter in these systems limit not only the frequency tuning range, but also the tuning speed. Recently, some dual-parallel polarization modulator (DP-PoIM) schemes have been proposed to generate frequency sextupling mm-wave signal without an optical filter, but lacks experimental demonstration[16,17].

In this paper, we firstly investigate a simplified optical mm-wave quadrupling scheme, which operates without either an electrical phase shifter or an optical filter. Compared with traditional optical mm-wave generation scheme, the new scheme exhibits a much broader frequency tunable range, lower wavelength dependence, and higher stability. The experiment results prove the gain of 6 GHz, 8 GHz and 10 GHz RF driving signals with an optical sideband suppression ratio (*OSSR*) of 15 dB and a radio frequency spurious suppression ratio (*RFSSR*) of 26 dB.

Fig.1 outlines the proposed scheme of frequency quadrupling optical mm-wave signal generation. The DP-MZM consists of two child MZMs (MZM-a and MZM-b) and a parent MZM (MZM-c).

* This work has been supported by the National Natural Science Foundation of China (Nos.61307099 and 11704293).

** E-mail: ccyun@126.com

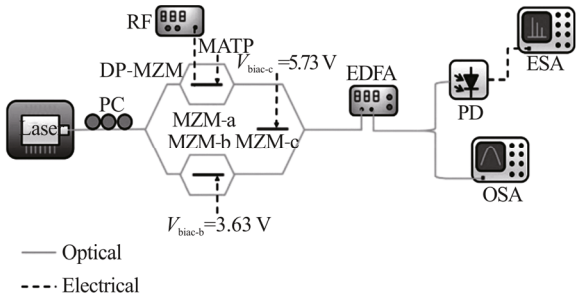

PC: polarization controller, DP-MZM: dual-parallel Mach-Zehnder modulator, RF: radio frequency generator, EDFA: erbium doped fiber amplifier, PD: photo-detector, ESA: electrical spectrum analyzer, OSA: optical spectrum analyzer

Fig.1 Principle diagram of the simplified optical mm-wave generation with frequency quadrupling

Assume the incident continuous wave has an expression

$$E(t)=E_0\exp\left\{\mathrm{j}\left[\omega_c t+\phi(t)\right]\right\}, \tag{1}$$

where E_0, ω_c and $\phi(t)$ are the amplitude, angular frequency and phase fluctuation of the optical field, respectively. In our scheme, the MZM-a biases at the maximum optical transmission point (MATP) to suppress all the odd-order optical sidebands. The output electrical field of the MZM-a has the form as

$$\begin{aligned}E_a=&\sqrt{\gamma}\exp(\mathrm{j}\omega_c t)\{\gamma\exp[\mathrm{j}\beta\cos(\omega_n t)]+\\&(1-\gamma)\exp[-\mathrm{j}\beta\cos(\omega_m t)]\}=\\&\sqrt{\gamma}\sum_{n=-\infty}^{\infty}(-1)^n J_{2n}(\beta)\exp[\mathrm{j}(\omega_c+2n\omega_m)t]+\\&\sqrt{\gamma}(1-2\gamma)\sum_{n=-\infty}^{\infty}(-1)^n J_{2n-1}(\beta)\exp\{\mathrm{j}[\omega_c+\\&(2n-1)\omega_m]t+\mathrm{j}\frac{\pi}{2}\},\end{aligned} \tag{2}$$

where $\beta=\pi V_m/2V_\pi$ is the modulation index (MI), V_m and ω_m are the amplitude and the angular frequency of the RF driving signal, V_π and γ are the switching voltage and the power splitting ratio of the DP-MZM, $J_n(\cdot)$ is the nth order Bessel function of the first kind.

There is no RF driving signal incident into MZM-b, and the optical carrier is DC biased at $V_{bias\text{-}b}$. The electrical field of the MZM-b output has a form as

$$\begin{aligned}E_b=&\sqrt{1-\gamma}\exp(\mathrm{j}\omega_c t)[\gamma\exp(\mathrm{j}\pi\frac{V_{bias\text{-}b}}{2V_\pi})+(1-\gamma)\cdot\\&\exp(-\mathrm{j}\pi\frac{V_{bias\text{-}b}}{2V_\pi})]=\\&[\sqrt{1-\gamma}\cos(\pi\frac{V_{bias\text{-}b}}{2V_\pi})]\exp(\mathrm{j}\omega_c t)+\sqrt{1-\gamma}\cdot\\&(2\gamma-1)\sin(\pi\frac{V_{bias\text{-}b}}{2V_\pi})]\exp[(\omega_c t+\frac{\pi}{2})\mathrm{j}]\cdot\end{aligned} \tag{3}$$

MZM-c is DC biased at $V_{bias\text{-}c}$ to introduce a phase difference into the output electrical fields of the MZM-a and the MZM-b. Ignoring the high order optical sideband terms, the output of the MZM-c has a form as

$$\begin{aligned}E_c=&E_a+E_b\approx\\&[\gamma J_0(\beta)+(1-\gamma)\cos(\pi\frac{V_{bias\text{-}b}}{2V_\pi})\exp(\mathrm{j}\pi\frac{V_{bias\text{-}c}}{V_\pi})]\cdot\\&\exp(\mathrm{j}\omega_c t)+[(1-\gamma)(2\gamma-1)\sin(\pi\frac{V_{bias\text{-}b}}{2V_\pi}).\\&\exp(\mathrm{j}\pi\frac{V_{bias\text{-}c}}{V_\pi})]\exp[(\omega_c t+\frac{\pi}{2})\mathrm{j}]-(1-2\gamma)\gamma J_1(\beta).\\&\{\exp[\mathrm{j}(\omega_c+\omega_m)t+\mathrm{j}\frac{\pi}{2}]+\exp[\mathrm{j}(\omega_c-\omega_m)t+\\&\mathrm{j}\frac{\pi}{2}]\}-\gamma J_2(\beta)\{\exp[\mathrm{j}(\omega_c+2\omega_m)t]+\\&[\mathrm{j}(\omega_c-2\omega_m)t]\}+(1-2\gamma)\gamma J_3(\beta).\\&\{\exp[\mathrm{j}(\omega_c+3\omega_m)t+\mathrm{j}\frac{\pi}{2}]+\exp[\mathrm{j}(\omega_c-3\omega_m)t+\\&\mathrm{j}\frac{\pi}{2}]\}+\gamma J_4(\beta)\{\exp[\mathrm{j}(\omega_c+4\omega_m)t]+\\&\exp[\mathrm{j}(\omega_c-4\omega_m)t]\}.\end{aligned} \tag{4}$$

According to Eq.(4), the optical carrier vanishes when the following conditions are satisfied,

$$\cos(\pi\frac{V_{bias\text{-}b}}{V_\pi})=1-\frac{1}{2\gamma(1-\gamma)}+\frac{\gamma^2 J_0^2(\beta)}{2\gamma(1-\gamma)^3}, \tag{5}$$

$$\tan(\pi\frac{V_{bias\text{-}c}}{V_\pi})=(2\gamma-1)\tan(\pi\frac{V_{bias\text{-}b}}{V_\pi}). \tag{6}$$

Assume γ=0.45, extinction ratios of single MZM and DP-MZM are 20 dB and 40 dB, respectively. Thus, Eqs.(5) and (6) lead to $V_{bias\text{-}b}$=3.63 V and $V_{bias\text{-}c}$=5.73 V.

The generated optical sideband signals cause beats when they arrive at the PD and generate the frequency quadrupling mm-wave signal from the two second-order optical sidebands. The photocurrent,

$$I_{PD}=\Re\,|E_c(t)|^2, \tag{7}$$

where $\Re$ is the responsivity of the PD.

In order to validate the quality of the frequency quadrupling mm-wave signal, we simulate the response of the system in Fig.1 on OptiSystem platform. The light source uses a continuous wave (CW) laser diode with central wavelength of 1 548.92 nm, linewidth of 10 MHz and output of +25 dBm. The MZM-a is driven by the RF driving signal of 10 GHz and biased at the MATP. The MZM-b and MZM-c are biased with the DC voltage set to 3.626 8 V and 5.734 9 V, respectively. In order to match with the actual experimental conditions, we reference the extinction ratio (*ER*) of DP-MZM (FUJITSU, FTM7962EP) in our experiment to that of MZM-a, MZM-b and MZM-c, which are 20 dB, 20 dB and 22 dB, respectively. An EDFA with gain of 20 dB and noise figure of 5 dB is utilized at the output of the DP-MZM for the insertion loss compensation of the DP-MZM. The responsivity of the PD is 0.8 A/W, dark current is 10 nA and thermal noise is 1×10^{-22} W/Hz.

The simulated optical spectrum of the DP-MZM for the frequency quadrupling mm-wave signal is shown in Fig.2. The resolution is 0.01 nm. The power of the

second-order optical sidebands is 8 dB, which is 15 dB higher than the first-order optical sidebands. The first-order optical sidebands are not suppressed completely due to the finite ER of the DP-MZM. Fig.3 illustrates the simulated electrical spectrum of the PD, in which 20 GHz harmonic and 40 GHz harmonic refers to the first-order and second-order optical sidebands. The power of the 40 GHz mm-wave signal is the strongest in the electrical spectrum with a 15 dBm electrical power and a 30 dB *RFSSR*.

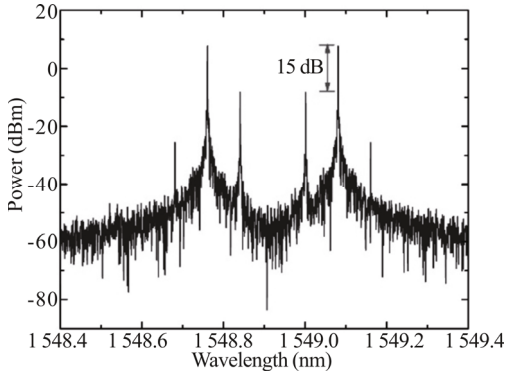

Fig.2 Simulated output optical spectrum of the DP-MZM

The ER of the single MZM is around 20—35 dB[18]. From Fig.4, we can see that the *OSSR* linear increases with the *ER*. The fitting result in Fig.4 shows the *OSSR* coefficient of the *ER* is 1.03. However, Fig.5 Shows the *RFSSR* linear increases with the ER before 31 dB and keeps even thereafter. The *RFSSR* is more sensitive to *ER* variation when it less than 31 dB at a gradient of 1.93 and keeps unchanged till 35 dB. The simulation results prove an acceptable system performance with *OSSR* over 15 dB and *RFSSR* over 30 dB on the condition of the *ER* of single MZM of 20 dB to 22 dB.

The experiment system shown in Fig.1 is exactly the same as in simulation. A distributed feedback Bragg (DFB) laser of 1 548.92 nm, linewidth of 3 MHz operates with a polarization controller (PC, THORLABS, FPC032) before launching into a DP-MZM (FUJITSU, FTM7962EP). DP-MZM has an insertion loss of 7 dB and an optical bandwidth of 22 GHz. A RF local oscillator (RF, ROHDE&SCHWARZ, SMB100A) supplies DP-MZM with RF signals. An EDFA amplifies the output signal of DP-MZM and sends into an optical spectrum analyzer (OSA, YOKOGAWA, AQ6370C). Finally, the frequency quadrupling mm-wave signal is detected by an integrated high-speed PD (40 GHz) and analyzed by an electrical spectrum analyzer (ESA, KEYSIGHT, N9010A, 10—44 GHz).

As analysis of the operation principle, MZM-a, MZM-b and MZM-c are biased at the MATP, the DC voltage of 3.63 V and 5.73 V, respectively. In order to obtain a stable DC voltage, we use the DC power supply of KEYSIGHT E3620A. In our experiments, we obtain 24 GHz, 32 GHz and 40 GHz mm-wave signal using a RF driving signal of 6 GHz, 8 GHz and 10 GHz.

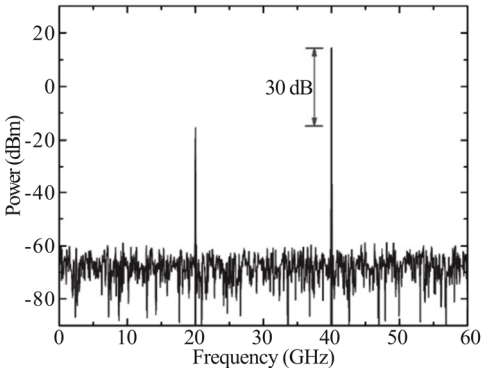

Fig.3 Simulated output electrical spectrum of the PD

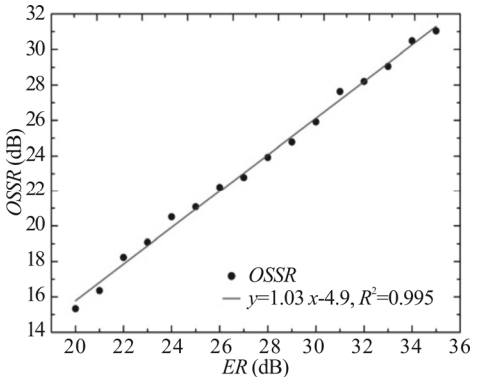

Fig.4 Impact of *ER* on *OSSR*

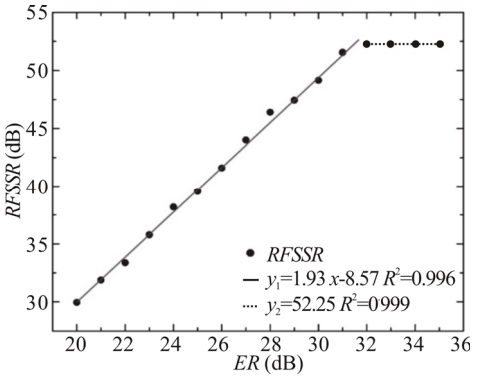

Fig.5 Impact of *ER* on *RFSSR*

Fig.6 shows the obtained optical spectrum of the DP-MZM. The wavelength resolution of the OSA is 0.02 nm. It is clearly shown in Fig.6 that the second-order optical sidebands have intervals of 24 GHz, 32 GHz and 40 GHz respectively for RF driving signal of 6 GHz, 8 GHz and 10 GHz, output power of +7 dBm and 15 dB *OSSR*. The results are in good consistency with the theoretical simulation results. Besides the second-order sidebands, several higher order harmonics remain observed for the imbalanced *y*-junction splitting ratio and imperfect ER of DP-MZM. Because a limited resolution of the OSA, measurement optical spectrum is smoother than simulated optical spectrum.

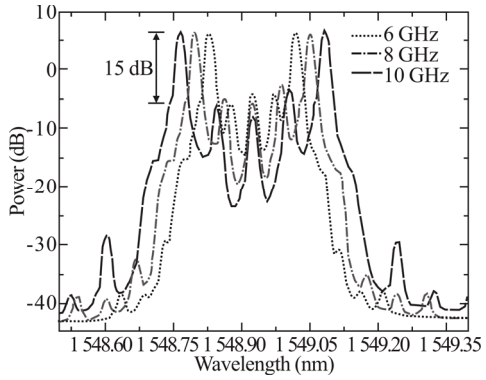

Fig.6 Measured optical spectra of the DP-MZM

Fig.7 shows the output electrical spectrum of the PD with 44 GHz span and 3 MHz resolution. The amplitudes of the strongest electrical output signals of 24 GHz, 32 GHz and 40 GHz are about four times that of the RF driving signals (6 GHz, 8 GHz and 10 GHz). The first, second and third terms of the electrical signal are effectively suppressed. The *RFSSR* of the generated quadrupling mm-wave signal is about 26 dB, which satisfies most practical applications.

In simulation, the RFSSR of proposed system is 30 dB. However, several factors degrade the final results to 26 dB. First, imperfect power splitting ratio of the 3 dB coupler sends uneven signals into the two arms of DP-MZM, which yields a finite *ER* and corrupts the suppression ratio[19]. The imbalance of the two arms of DP-MZM is the cause for other undesired optical sidebands. In Fig.6, we find the first-order optical sidebands and the optical carrier are not fully suppressed. Second, a considerable bias drift of DP-MZM and sensitive optical transmission point require dynamic compensation of bias drift with an automatically controlling circuit[12]. By using fine quality components and feedback controlling circuit, the bias drift and transmission point might realize precise control. Third, an accurate control of the MI can influence the *OSSR* and RFSSR of the generated frequency quadrupling mm-wave signal[12]. According to Eq.(2), $\beta=\pi V_m/2V_\pi$, V_m is the amplitude of the RF driving signal. By using stable RF local oscillator, the MI might improvement.

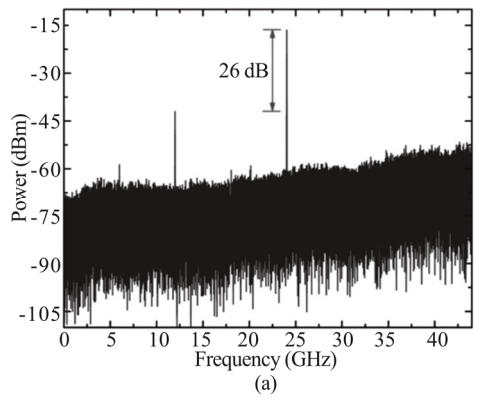

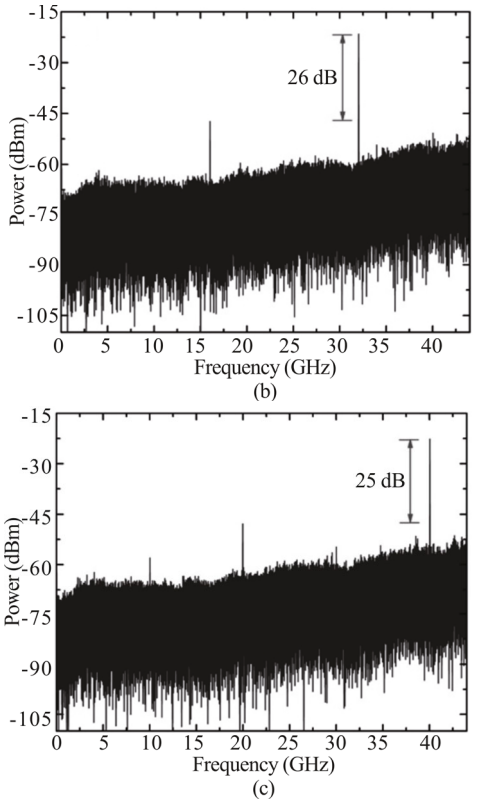

Fig.7 Measured electrical spectra of the PD: (a) 6 GHz RF driving signal; (b) 8 GHz RF driving signal; (c) 10 GHz RF driving signal

In this paper, a simplified frequency quadrupling configuration for optical mm-wave generation is proposed, analyzed, and demonstrated. The proposed scheme without any electrical phase shifter and optical filter. According to the theoretical analysis and the computer simulation, a 40 GHz mm-wave signal with the *OSSR* and *RFSSR* of 15 dB and 30 dB is generated from a 10 GHz RF driving signal. Then, the impact of the *ER* on the *OSSR* and *RFSSR* is investigated in this paper. Furthermore, Experiments prove an *OSSR* of 15 dB and *RFSSR* of 26 dB for the new frequency quadrupling scheme at 6 GHz, 8 GHz and 10 GHz RF driving signal. Since without electrical phase shifter and optical filter in this system, the proposed scheme is particularly attractive for broadband wireless communications, ROF systems and continuously tunable mm-wave signal generation.

References

[1] S.H. Jang, B.H. Park and S.C Hong, Opt. Express **25**, 8335 (2017).

[2] R.M. Li, W.Z. Li, M.L. Ding, Z.L. Wen, Y.L. Li, L.J. Zhou, S.S. Yu, T.H. Xing, B.W. Gao, Y.C. Luan, Y.T. Zhu, P. Guo, Y. Tian and X.D. Liang, Opt. Express **25**, 14334 (2017).

[3] F.S. Vieira, F.C. Cruz, D.F. Plusquellic and S.A. Diddams, Opt. Express **24,** 30100 (2016).

[4] F.Z. Zhang, X.Z. Ge, B.D. Gao and S.L. Pan, Opt. Express **23**, 21868 (2015).

[5] S. Deng, M. Li, H.Y. Gao and Y.W. Dai, Opt. Fiber Technol. **31**, 156 (2016).

[6] J.J. O'Reilly, P.M. Lane, R. Heidemann and R. Hofstetter, Electron. Lett. **28**, 2309 (1992).

[7] J. Zhang, H.W. Chen, M.H. Chen, T.L. Wang and S.Z. Xie, IEEE Photon. Technol. Lett. **19**, 1057 (2007).

[8] J. Zhang, M.G. Wang, C.G. Shao, T.J. Li and S.S. Jian, Acta Optic Sin. **3**, 306004 (2014). (in Chinese)

[9] W.J. Jiang, C.T. Lin, H.S. Huang, P.T. Shih, J. Chen and S. Chi, 60-GHz Photonic Vector Signal Generation Employing Frequency Quadrupling Scheme for Radio-over-Fiber Link, Optical Fiber Communication Conference and National Fiber Optic Engineers Conference, OWF1 (2009).

[10] J. Zhang, H.W. Chen, M.H. Chen, T.L. Wang and S.Z. Xie, Opt. Lett. **32**, 1020 (2007).

[11] M. Mohamed, X.P. Zhang, B.C. Hraimel and K. Wu, Opt. Express **16**, 10141 (2008).

[12] Y.Y. Gao, A.J. Wen, Q.W. Yu, N.N. Li, G.B. Lin, S.Y. Xiang and L. Shang, IEEE Photon. Technol. Lett. **26**, 1199 (2014).

[13] A. Kumar and V. Priye, Appl. Opt. **22**, 5830 (2016).

[14] Z.H. Zhu, S.H. Zhao, W.Z. Zhao, W. Wang and B.Q. Lin, Appl. Opt. **32**, 9432 (2015).

[15] Z.H. Zhu, S.H. Zhao, X.C. Chu and Y. Dong, Opt. Commun. **354**, 40 (2015).

[16] Z.H. Zhu, S.H. Zhao, X. Li, K. Qu and T. Lin, Opt. Laser Technol. **87**, 1 (2017).

[17] Z. Zhu, S. Zhao, X. Li, K. Qu and T. Lin, Opt. Laser Technol. **90**, 144 (2017).

[18] P.M. Shi, S. Yu, Z.K. Li, S.G. Huang, J. Shen, Y.J. Qiao, J. Zhang and W.Y. Gu, Opt. Fiber Technol. **17**, 236 (2011).

[19] Y. Qin, J.Q. Sun, M.D. Du and J.F. Liao, Opt. Commun. **315**, 280 (2014).